Supporting information

Multivacant polyoxometalate-stabilizing palladium nanoparticles catalyzes N-formylation of amines with CO_2 and H_2

Wenkai Lai,[a] Yongjun Jiang,[b] Huiying Liao,[a] Xinjia Wei,[a] Zhiwei Xu,[a] Ji Ding,[a] Ning An,[a] Sheng Dai[b] and Zhenshan Hou *,[a]

[a]State Key Laboratory of Green Chemical Engineering and Industrial Catalysis, Research Institute of Industrial Catalysis, School of Chemistry & Molecular Engineering, East China University of Science and Technology, Shanghai 200237, China.

[b]Key Laboratory for Advanced Materials and Feringa Nobel Prize Scientist Joint Research Center, Institute of Fine Chemicals, School of Chemistry & Molecular Engineering, East China University of Science and Technology, Shanghai 200237, China.

*Corresponding author at: State Key Laboratory of Green Chemical Engineering and Industrial Catalysis, Research Institute of Industrial Catalysis, School of Chemistry & Molecular Engineering, East China University of Science and Technology, Shanghai 200237, China.

Email address: houzhenshan@ecust.edu.cn. (Z. Hou)

Experimental section

1. Materials

All commercially available chemicals and solvents were used as received without further purification. Palladium chloride ($PdCl_2$) Sodium metasilicate ($Na_2SiO_3 \cdot 9H_2O$) and sodium tungstate ($Na_2WO_4 \cdot 2H_2O$) were obtained from Shanghai D&B Biological Science and Technology Co., Ltd. sodium phenoxide, Potassium chloride (KCl), Potassium phenolate, potassium carbonate (K_2CO_3) and other base were obtained from Sinopharm Chemical Reagent Co., Ltd. Morpholine (AR) and other amine derivatives were purchased from Aladdin Industrial Corporation. All organic solvents and other materials were purchased from Shanghai Titan Scientific Co., Ltd. and Adamas-beta reagent. High purity H_2 (99.999%) and CO_2 (>99.95%) was supplied by Shanghai Shangnong Gas Co., Ltd. $^{13}CO_2$ (99 atom% ^{13}C, 99.93 atom % ^{16}O) gas was purchased from Sigma-Aldrich Co., Ltd.

2. Catalyst characterization

ICP-AES analysis of Si, W, Pd, K was performed on a TJA IRIS 1000 instrument. Powder X-ray diffraction (XRD) patterns were performed in the 2θ range of 5-75° from Rigaku equipped with a 9 kW rotating anode Cu source at 45 kV and 100 mA. UV-vis spectra were measured using a Varian Cary 500 spectrophotometer. Fourier-transform FT-IR spectra was recorded from pressed KBr pellets at room temperature on a Nicolet Nexus 670 FT-IR spectrometer. Scanning transmission electron microscopy (STEM) characterization was performed on a ThermoFisher Talos F200X microscope under 200 kV. High angle annular dark field (HAADF)-STEM images were recorded using a convergence semi angle of 10.5 mrad, and inner- and outer collection angles of 59 and 200 mrad, respectively. UV-vis spectra were measured using a Varian Cary 500 spectrophotometer. Electrospray ionization time-of-flight mass (ESI-TOF-MS) spectra was recorded in the negative mode on an Agilent 6520 Q-TOF LC/MS mass spectrometer. The sample was dissolved in methanol (CH_3OH) and directly injected into the chamber at 20 μL·min-1. Typical instrument parameters: capillary voltage, 4000 V; nebulizer, 1.0 bars; dry gas, 6.0 L·min-1 at 120 °C; m/z

range, 500-3000. X-ray photoelectron spectroscopy (XPS) was performed using Thermo ESCALAB 250. ^{1}H NMR were recorded on a Bruker Avance III 400 instrument (400 MHz for ^{1}H NMR) and ^{13}C NMR were recorded on Ascend 600 (151 MHz for ^{13}C NMR) using methanol-d_4, chloroform-d_1 and DMSO-d_6 as solvents.

In-situ FT-IR spectra were collected at 140 ^{o}C with a Nicolet Nexus 670 spectrometer equipped with a MCT detector and a high temperature reaction chamber with ZnS windows. The solid samples were prepared with KBr pressed-disk technique. The in-situ FT-IR spectra were collected in the range of 4000-650 cm^{-1} by accumulating 16 scans at a 4 cm^{-1} resolution. Background spectra were recorded in flowing N_2 at the rate of 10 sccm for 0.5 h at 140 ^{o}C and subtracted from the sample spectrum for each measurement. Nicolet OMNIC software was used to convert the absorbance data into Kubelka-Munk (KM) format. *In situ* FT-IR spectra of the samples were then obtained.

3. Catalyst preparation

3.1 Preparation of $K_8SiW_{11}O_{39}\cdot 13H_2O$ (SiW_{11})

SiW_{11} was prepared according to a similar procedure as reported.[1] $Na_2SiO_3\cdot 9H_2O$ 2.842 g (10 mmol) was dissolved in 10 mL distilled water at room temperature (Solution A). In a 250 mL beaker, $Na_2WO_4\cdot 2H_2O$ 36.284 g (0.11 mol) was dissolved in 30 mL boiling distilled water (Solution B). Under vigorous stirring, 40 mL HCl solution (include 8 mL 36%-38% HCl) was added dropwise to the boiling solution B and stirred 30 min subsequently. Solution A was then added, followed by quick addition of another 17 mL HCl (include 7 mL 36%-38% HCl). The pH reading was adjusted to 4.95. The solution was kept boiling for 1 h. After cooling to room temperature, 30 g KCl was added to the solution and stirred shortly. The white solid product was collected by filtration, washed with two 10 mL portions of a KCl solution (1 M) followed by two 10 mL portions of cold water. The white solid was obtained and recrystallized from 50 mL 80^{o}C water. The white crystalline product was dried under vacuum for 24 h at 60 ^{o}C. Yield: 23.7 g (73.6% based on W). FT-IR: 1628 and 3436 cm^{-1} (ν O-H), 997 cm^{-1} (ν_{as} Si−O_a), 958 cm^{-1} (ν_{as} W=O_d), 889 cm^{-1} (ν_{as}

W−O_b−W), 796 and 727 cm^{-1} (ν_{as} W−O_c−W) (Fig. 2).

3.2 Preparation of $K_{10}SiW_9O_{34}$ (SiW_9)

SiW_9 was prepared according to a similar procedure as reported.[2] 18.2 g (55 mmol) of $Na_2WO_4 \cdot 2H_2O$ and 1.43 g $Na_2SiO_3 \cdot 9H_2O$ (5 mmol) was dissolved in 20 ml of distilled water at 100 °C. Slowly add 13 ml of 6 M HCl and stirred vigorously. The clear reaction mixture was concentrated to 30mL its solvent volume at 100 °C. After cooling to room temperature, SiO_2 precipitate was centrifuged off. 5g K_2CO_3 was dissolved in 15 ml of distilled water. Slowly add 15 mL K_2CO_3 solution into the clear reaction mixture and stirred 2h slowly. The white solid product was collected by filtration, washed with two 10 mL portions of a KCl solution (1 M) followed by two 10 mL portions of cold water. And the white product was dried under vacuum for 24 h at 40 °C. Yield: 11.5 g (73.6% based on $Na_2SiO_3 \cdot 9H_2O$). FT-IR: 1628 and 3436 cm^{-1} (ν O-H), 1058 and 985 cm^{-1} (ν_{as} Si−O_a), 939 cm^{-1} (ν_{as} W=O_d), 861 cm^{-1} (ν_{as} W−O_b−W), 799 and 715 cm^{-1} (ν_{as} W−O_c−W) (Fig. 2).

3.3 Preparation of $K_6SiW_{11}O_{39}Pd \cdot nH_2O$ (Pd^{II}-SiW_{11}).

Pd^{II}-SiW_{11} was prepared according to a similar procedure as reported.[3] $PdCl_2$ (0.55 mmol, 98 mg) was dispersed in 20 mL deionized water, and then the suspension was added dropwise to a 90 °C solution of $K_8SiW_{11}O_{39} \cdot 13H_2O$ (0.5 mmol, 1.61 g, 20 mL H_2O). The pH of the mixture was about 5.5, then solution was adjusted pH to 5.0 with acetic acid and stirred for 0.5 h at 90 °C. After the mixture was cooled down, 20 mL methanol was added and precipitate was obtained. The pale brown solid was collected after vacuum drying. Yield: 0.94 g (63% based on W). FT-IR: 1628 and 3436 cm^{-1} (ν O-H), 995 cm^{-1} (ν_{as} Si−O_a), 955 cm^{-1} (ν_{as} W=O_d), 891 cm^{-1} (ν_{as} W−O_b−W), 796 and 727 cm^{-1} (ν_{as} W−O_c−W) (Fig. 2).

3.4 Preparation of $K_{12}[Pd_3(SiW_9O_{34})_2] \cdot nH_2O$ (Pd^{II}-SiW_9)

Pd^{II}-SiW_9 was prepared according to a similar procedure as reported.[4] $PdCl_2$ (0.55 mmol, 100 mg) was dispersed in 20 mL deionized water. Then 1.00 g (0.33 mmol) of

SW_9 was added slowly, with vigorous stirring. The pH was adjusted to 4.8 with aqueous Na_2CO_3 (1 M) and the resulting solution was heated to 80 °C for 1 h and then cooled to room temperature. After cooling, the solution was centrifuged and filtered to remove all possible impurities and unreacted compounds. Solid KCl (1.0 g, 13 mmol) was added with stirring and a precipitate was formed immediately. The product was filtered off, yielding a dark brown solid as the Pd^{II}-SiW_9. Yield: 0.436 g (37% based on W). FT-IR: 1628 and 3436 cm^{-1} (ν O-H), 1081 cm^{-1} (ν_{as} Si−O_a), 946 cm^{-1} (ν_{as} W=O_d), 892 cm^{-1} (ν_{as} W−O_b−W), 773 and 710 cm^{-1} (ν_{as} W−O_c−W) (Fig. 2).

3.5 Preparation of POM-stabilizing Pd nanoparticles

3.5.1 Preparation of Pd^0-SiW_{11}

0.2g Pd^{II}-SiW_{11} was mixed with 5 mL MeOH in a 50 mL stainless steel autoclave equipped with a magnetic bar. Then the autoclave was charged with 3 MPa H_2 and heated at 140 °C for 12h under the stirring conditions. After cooling down the autoclave and release the H_2 slowly, the suspension was filtrated out and the resulting black powder was designated as the reduced *catalyst (Pd^0-SiW_{11})*. Yield: 0.2 g (>95%). FT-IR: 1628 and 3436 cm^{-1} (ν O-H), 996 cm^{-1} (ν_{as} Si−O_a), 956 cm^{-1} (ν_{as} W=O_d), 890 cm^{-1} (ν_{as} W−O_b−W), 796 and 727 cm^{-1} (ν_{as} W−O_c−W) (Fig. 2).

3.5.2 Preparation of Pd^0-SiW_9

0.2g Pd^{II}-SiW_9 was mixed with 5 mL MeOH in a 50 mL stainless steel autoclave equipped with a magnetic bar. Then the autoclave was charged with 3 MPa H_2 and heated at 140 °C for 12h under the stirring conditions. After cooling down the autoclave and release the H_2 slowly, the suspension was filtrated out and the resulting black powder was designated as the reduced *catalyst (Pd^0-SiW_9)*. Yield: 0.2 g (>95%). FT-IR: 1628 and 3436 cm^{-1} (ν O-H), 1078 cm^{-1} (ν_{as} Si−O_a), 948 cm^{-1} (ν_{as} W=O_d), 894 cm^{-1} (ν_{as} W−O_b−W), 799 and 725 cm^{-1} (ν_{as} W−O_c−W) (Fig. 2).

4. Preparation of potassium methyl carbonate

Into a 50 ml schlenk flask, provided with a mechanical stirrer, and a gas-inlet tube

whose top was connected to a calcium chloride tube, were placed potassium phenolate (0.35 g, 3 mmol), anhydrous methanol (0.5 ml), and anhydrous acetone (5 ml, as a solvent of sodium phenoxide). A suffcient volume of dry carbon dioxide was slowly introduced into the stirred acetone solution and white precipitates soon formed. These precipitates were collected on a glass filter, washed with dry ether, and then dried in vacuo at room temperature. Yield: 0.24 g (72.5% based on potassium phenolate).

5. The kinetic reaction of N-formylation reaction of morpholine with CO_2 and H_2

The general reaction rate equation of N-Formylation of amines with CO_2 and H_2 can be expressed by the following formula (3), in which the r, $[C_m]$, [cat.] and $[H_2]$ represent reaction rate, the concentration of morpholine at time of t, catalyst concentration, hydrogen pressure, respectively. Formula (1) can be simplified to (2) due to the catalysts and hydrogen were excessive in the reaction system. Assuming the reaction was a first-order reaction (γ= 1), (2) can be expressed as (3) or (4), c_0, c_t and X represent initial concentration of morpholine, concentration and conversion of morpholine at time of t. Formula (4) finally was expressed as equation (5).

$$r = -d[C_m]/dt = k_1 * [cat.]^{\alpha} * [H_2]^{\beta} * [C_m]^{\gamma} \quad (1)$$

$$-d[C_m]/dt = k * [C_m]^{\gamma},\ k = k_1 * [cat.]^{\alpha} * [H_2]^{\beta} \quad (2)$$

$$-d[C_m]/dt = k * [C_m] \quad (3)$$

$$\ln (c_0/c_t) = kt,\ c_t = c_0 * (1-X) \quad (4)$$

$$\ln (1-X) = -kt \quad (5)$$

6. The quantitative analysis of CO and HCOOMe from CO_2 and H_2

The reaction was carried out in a 50 mL stainless steel autoclave equipped with a magnetic bar. In the experiment, Pd^0-SW_9 (40 mg), K_2CO_3 (0.7 mmol) and methanol (5 mL) were sequentially added into the high-pressure stainless steel reactor and sealed. The CO_2 was charged into the reactor three times to remove the air. After that, the reactor was charged with CO_2 and H_2 to the desired pressure and heated to the preset temperature under continuous stirring condition. After reaction, the mixed gas was collected using a gas bag, and subjected to GC analysis quipped TCD detector

(external standard method). The amount of CO was calculated as follows (Equations 6), in which the V, R, and T represent the volume of mixed gas (mL), the Gas Constant, and room temperature (K), respectively:

$$Amount\ of\ CO\ (mole) = \frac{partial\ pressure\ of\ CO\ (MPa)\ \times\ V}{RT} \times 100\%$$

(6)

Meanwhile, the products and residual reactants were distributed in the methanol phase. After methanol phase was removed, the catalysts were then washed and extracted with fresh methanol (2×3 mL). The methanol phase was combined and subjected to GC and GC-MS analysis (mesitylene as internal standard). The amount of HCOOMe was calculated as follows (Equations 7), in which the $[A_s]$, $[A_p]$, and [K] represent the GC area of internal standard, the GC area of product, and correction factor, respectively:

$$Amount\ of\ product\ (mole) = \frac{amount\ of\ internal\ standard\ (mole)\ \times [Ap]}{[As]} \times [K] \times 100\%$$

(7)

Table S1. Elemental analysis of the POM-based catalysts[a]

Catalysts		Si / %	W / %	K / %	Pd / %
Pd^{II}-SiW_{11}	Calculated	0.93	60.99	7.76	3.53
	Found	0.95	60.93	7.81	3.50
Pd^{II}-SiW_9	Calculated	1.08	63.15	8.95	6.09
	Found	1.11	63.32	9.05	6.07
Pd^0-SiW_{11}	Found	0.97	61.13	7.85	3.56
Pd^0-SiW_9	Found	1.18	64.20	9.13	6.11
spent Pd^0-SiW_9	Found	1.27	65.35	9.14	6.05

[a]The contents of Si, W, K and Pd were measured by AES-ICP.

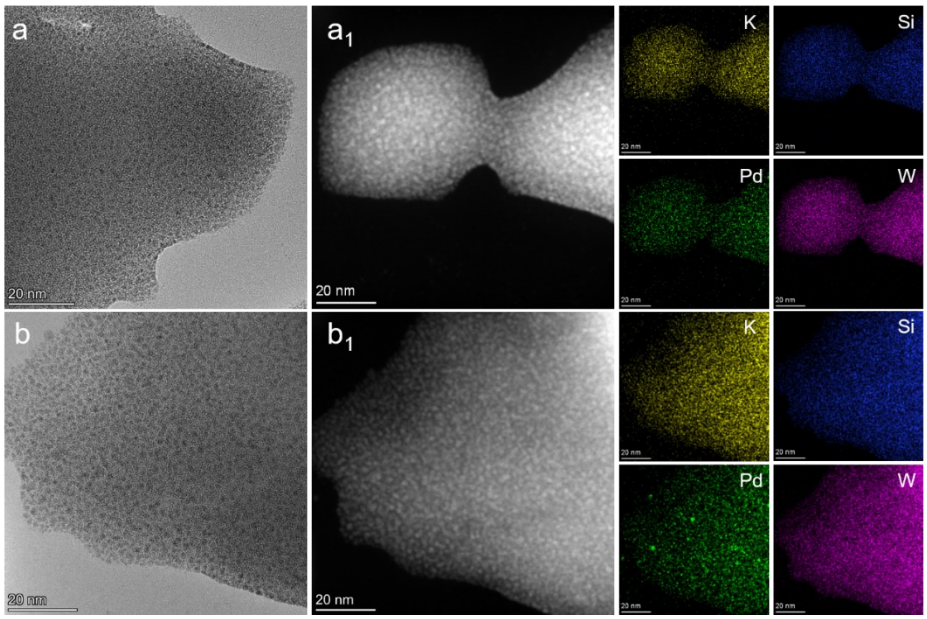

Fig. S1. HR-TEM images of (a) Pd^{II}-SiW_{11}, and (b) Pd^{0}-SiW_{11}. STEM images of (a_1) Pd^{II}-SiW_{11}, and (b_1) Pd^{0}-SiW_{11} catalyst and the corresponding elemental maps of K, Si, Pd, and W.

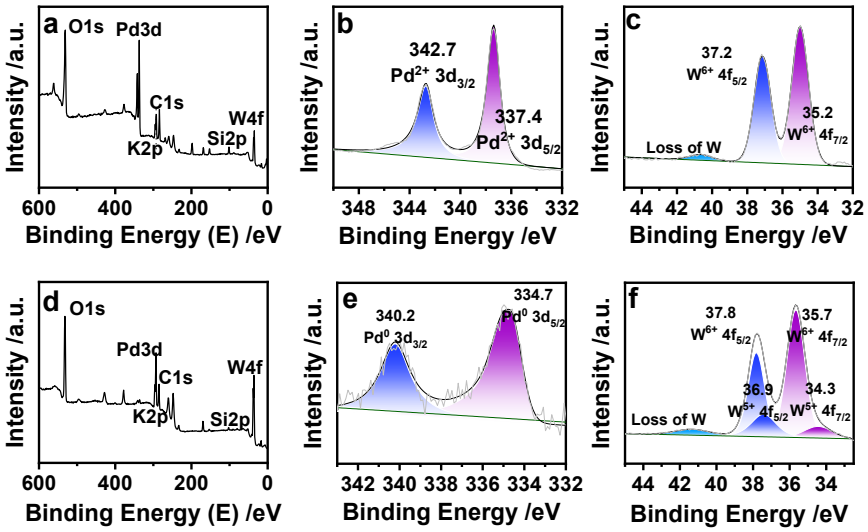

Fig. S2. XPS survey spectra, Pd 3d XPS spectra, and W 4f XPS spectra of Pd^{II}-SiW_{11} (a-c) and Pd^{0}-SiW_{11} (d-f).

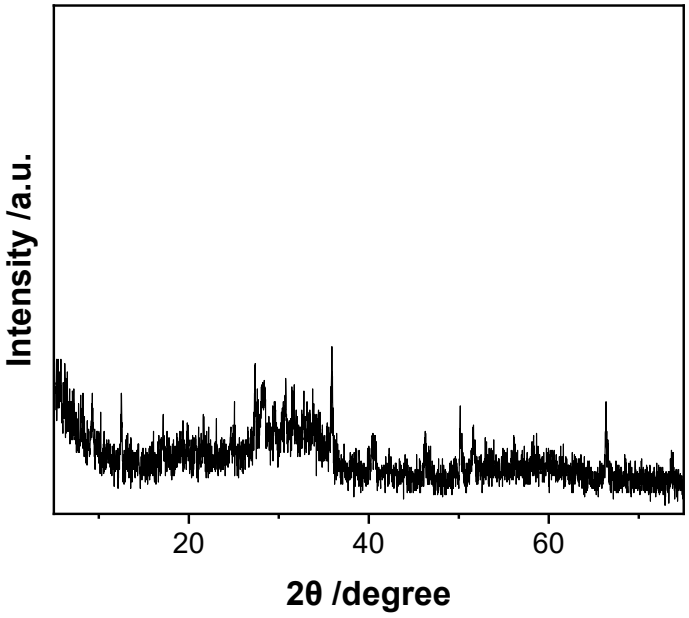

Fig. S3 XRD spectra of the spent Pd^0-SiW_{11} catalyst.

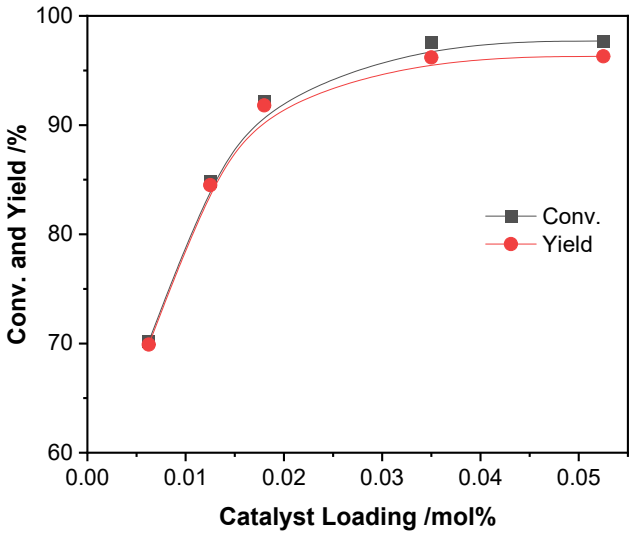

Fig. S4. Optimization of reaction parameters on N-formylation of morpholine. Reaction conditions: 4 mmol morpholine, Pd^0-SiW_9 as catalyst, 5 mL of MeOH, and 0.7 mmol K_2CO_3, 140 °C, 3.0 MPa CO_2, 3.0 MPa H_2, and 12 h.

Table S2 N-formylation of morpholine to formamide with CO_2/H_2 in different solvents.

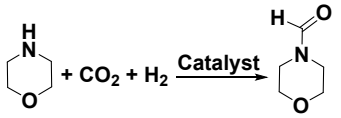

Entry	Solvents	Conv./%	Yield/%
1	n-Hexane	5.3	4.9
2	THF	36.8	36.2
3	MeCN	17.0	16.7
4	Toluene	47.6	45.3
5	EtOH	44.3	41.7
6	i-PrOH	64.9	62.1
7	MeOH	>99	>99
8[a]	MeOH	none	none

Reaction conditions: morpholine 5 mmol, 0.035 mol% catalyst, base 0.7 mmol, CO_2 3 MPa, H_2 3 MPa, 140 °C, MeOH 5 mL, and 12 h. [a]Without H_2.

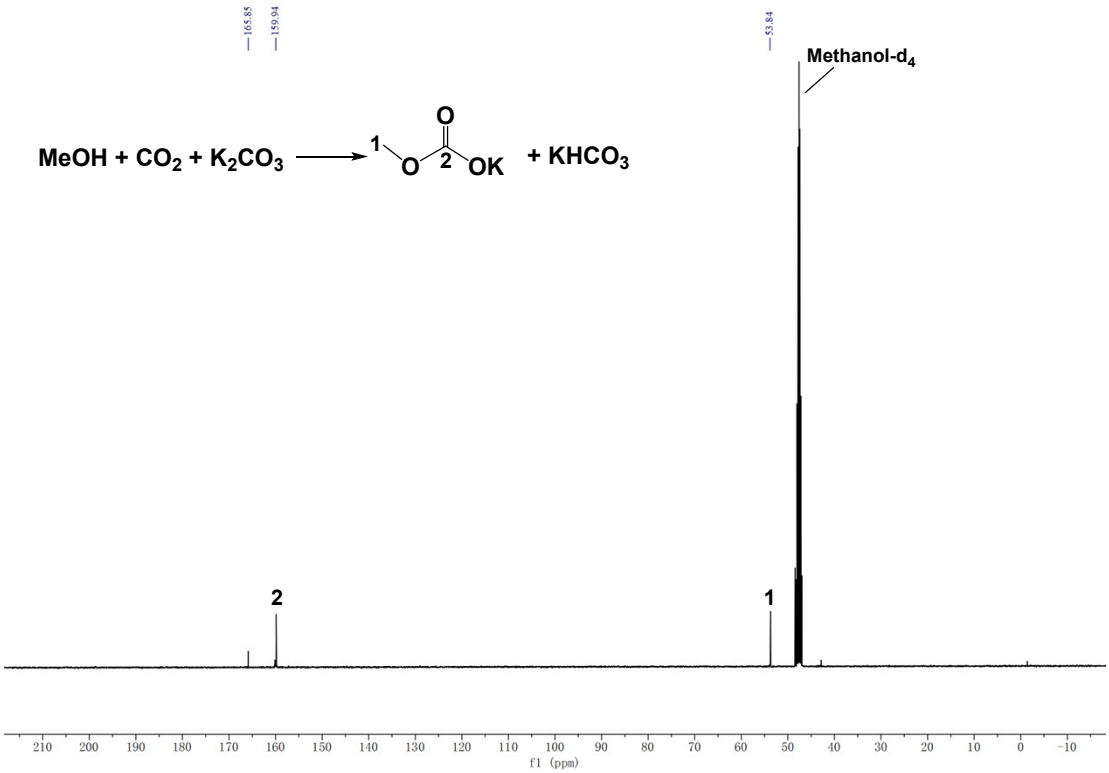

Fig. S5. ^{13}C NMR of the mixture obtained from the CO_2, methanol-d_4 and K_2CO_3.

Potassium methyl carbonate: white solid. ^{1}H NMR (400 MHz, methanol-d_4) δ 2.86 (s, 3H) ^{13}C NMR (151 MHz, methanol-d_4) δ 159.68, 53.95.

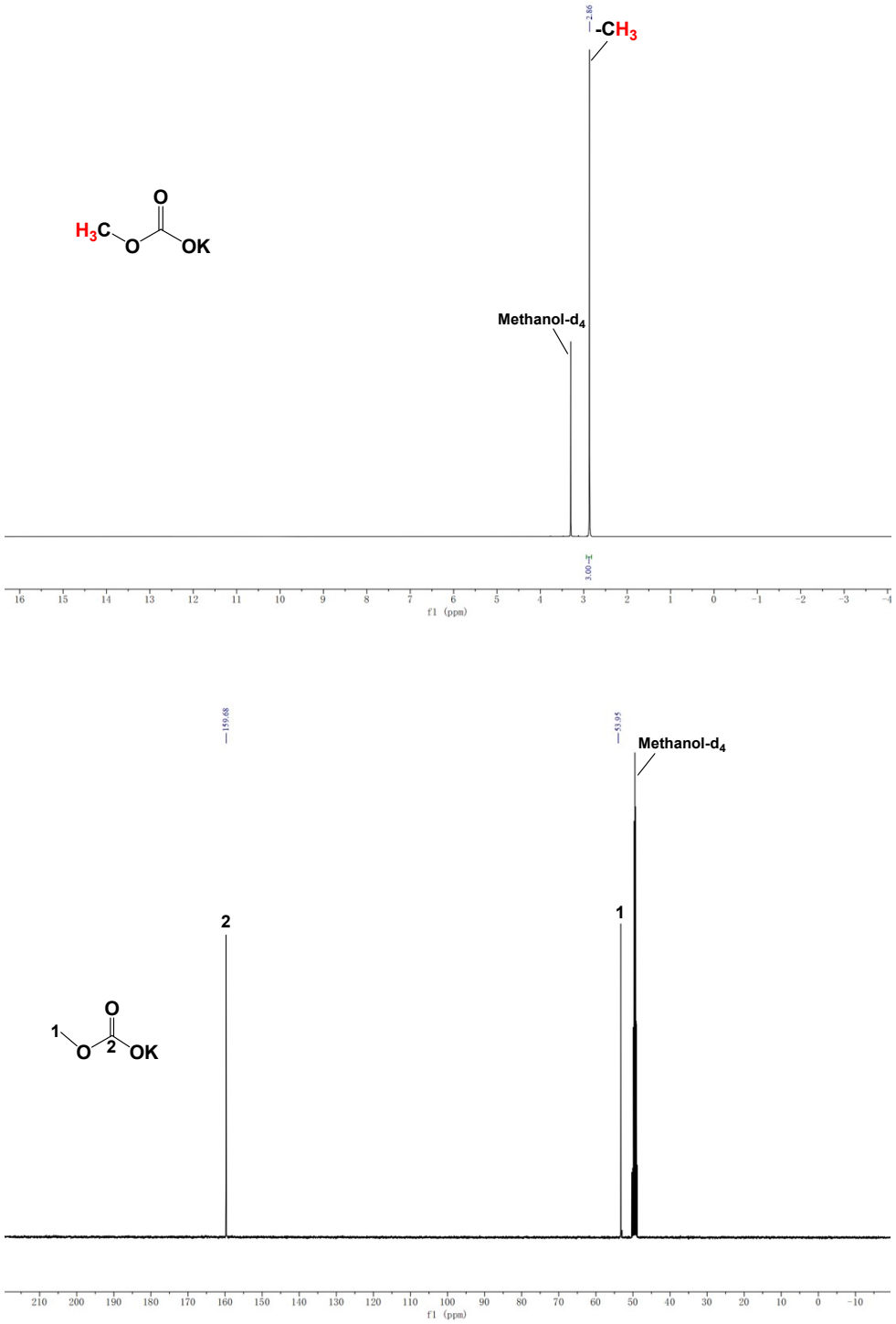

Fig. S6. ^{1}H NMR (upper) and ^{13}C NMR (bottom) spectra of potassium methyl carbonate in methanol-d_4.

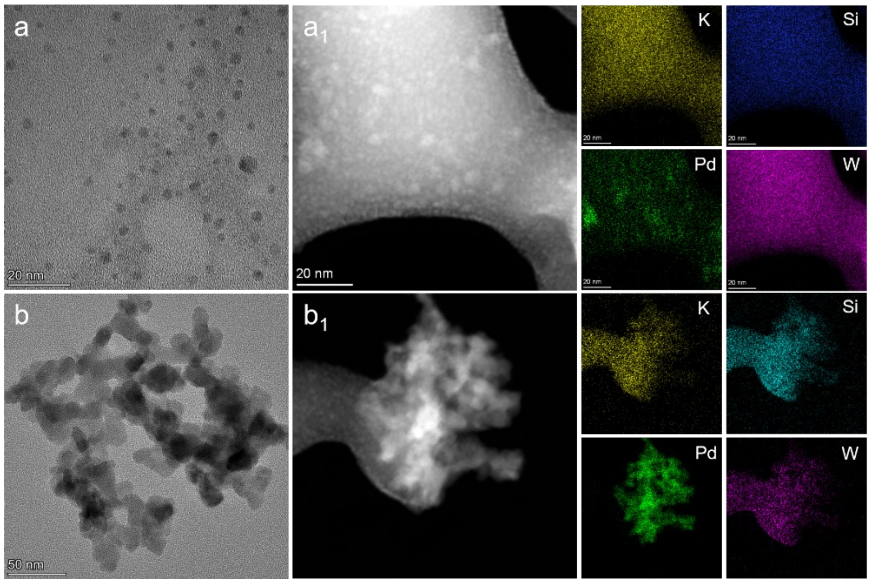

Fig. S7. HR-TEM images of (a) Pd^0-SiW_9 catalyst after eight runs, and (b) Pd^0-SiW_{11} catalyst after one run. STEM images of (a_1) Pd^0-SiW_9 catalyst after eight runs, and (b_1) Pd^0-SiW_{11} catalyst after one run and the corresponding elemental maps of K, Si, Pd, and W.

Table S3. Comparison of the present catalytic system with the previous reports in N-formylation reaction

Catalysts	T /°C	CO_2/H_2 /MPa	t /h	Solvent	Yield/ %	Ref.
Pd/C-3	130	1/3	24	MeOH	99	5
Pd-LDH	140	3/3	16	MeOH	91	6
Pd−Au/PANI-CNT	125	3.5/3.5	48	1,4-dioxane	95	7
Pd/Al_2O_3-NR-RD	130	1/2	24	octane	96	8
Imine-POP@Pd	100	3/3	24	DMI	97	9
Au/TiO_2	120	2/3	5	DMA	99	10
CarCMP-1@Ru	130	4/4	24	MeOH	91	11
Ir/ND@G	150	2.5/2.5	96	1,4-dioxane	64.5	12
BMIMOAc_Ru-ZrP	140	3/3	14	4.9	92	13
Pd^0-SiW_9	140	3/3	12	MeOH	98	In this work

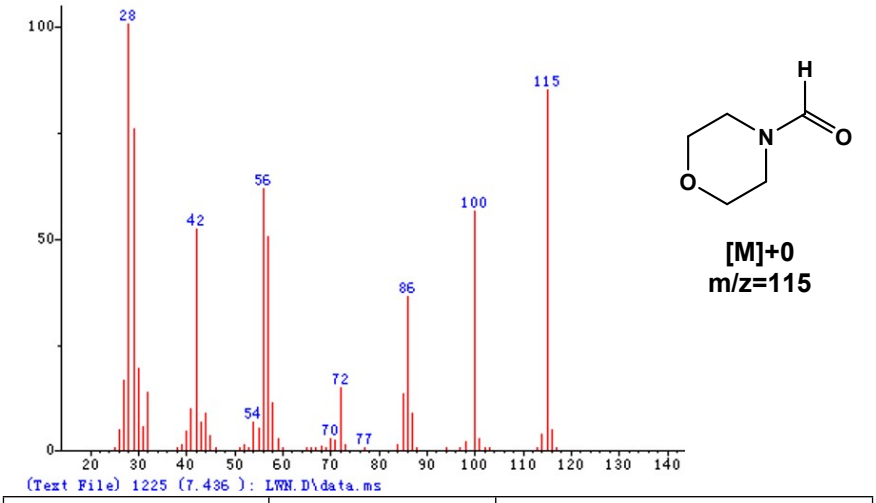

EI detected species	m/z value	Relative Natural Abundance (%)
[M]+0	115	100.00
[M]+1	116	6.22

Fig. S8. EI-MS spectra of N-formylmorpholine.

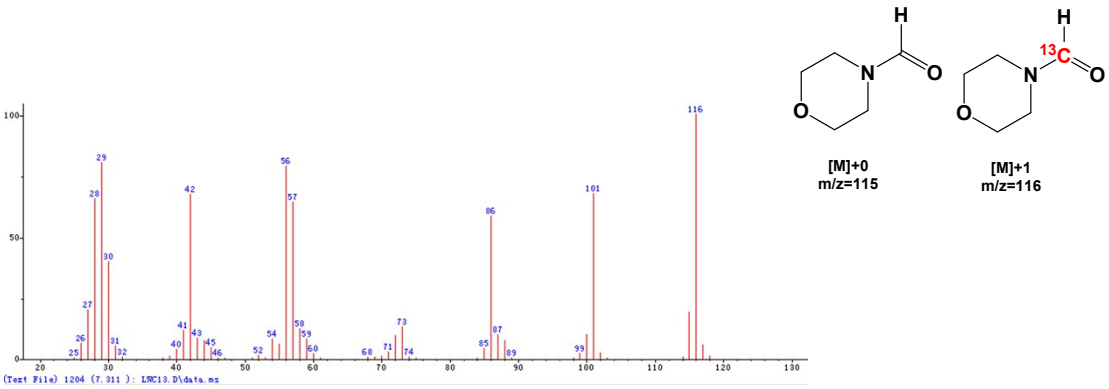

EI detected species	m/z value	Relative Natural Abundance (%)	Observed Abundance (%)	Corrected Abundance (%)	Isotopic Enrichment Relative (%)
[M]+0	115	100	12.07	12.07	11
[M]+1	116	6.22	93.39	92.67	89

Fig. S9. EI-MS spectra of N-formylmorpholine.

The corrected abundance (%) of [M]+1 = 93.39%−12.07%×6.22% = 92.67%;

The isotopic enrichment relative (%) of [M]+0 = 12.07/(12.07+92.67)×100% = 11.5%;

The isotopic enrichment relative (%) of [M]+1 = 92.67/(12.07+92.67)×100% = 88.5%.

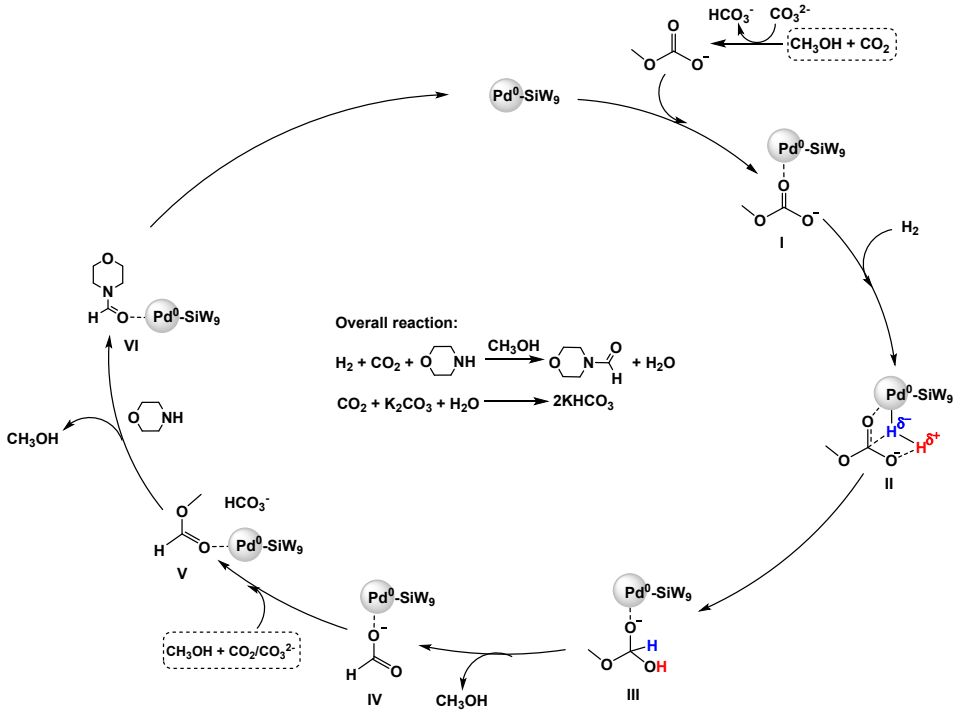

Fig. S10. Possible reaction pathway on Pd^0-SiW_9 catalyst with K_2CO_3 in N-formylation reaction (K^+ has been omitted for the clarity).

N, N-diethylformamide, colorless liquid, purification by reduced pressure distillation. ^{1}H NMR (400 MHz, DMSO-d_6) δ 8.40 (minor isomer, s, 0.50H), 7.98 (major isomer, s, 0.53H), 3.25 (dq, 3H), 2.86 (m, 1H), 1.08 (m, 6H). ^{13}C NMR (151 MHz, DMSO-d_6) δ 162.41, 41.38, 41.28, 13.01, 11.38.

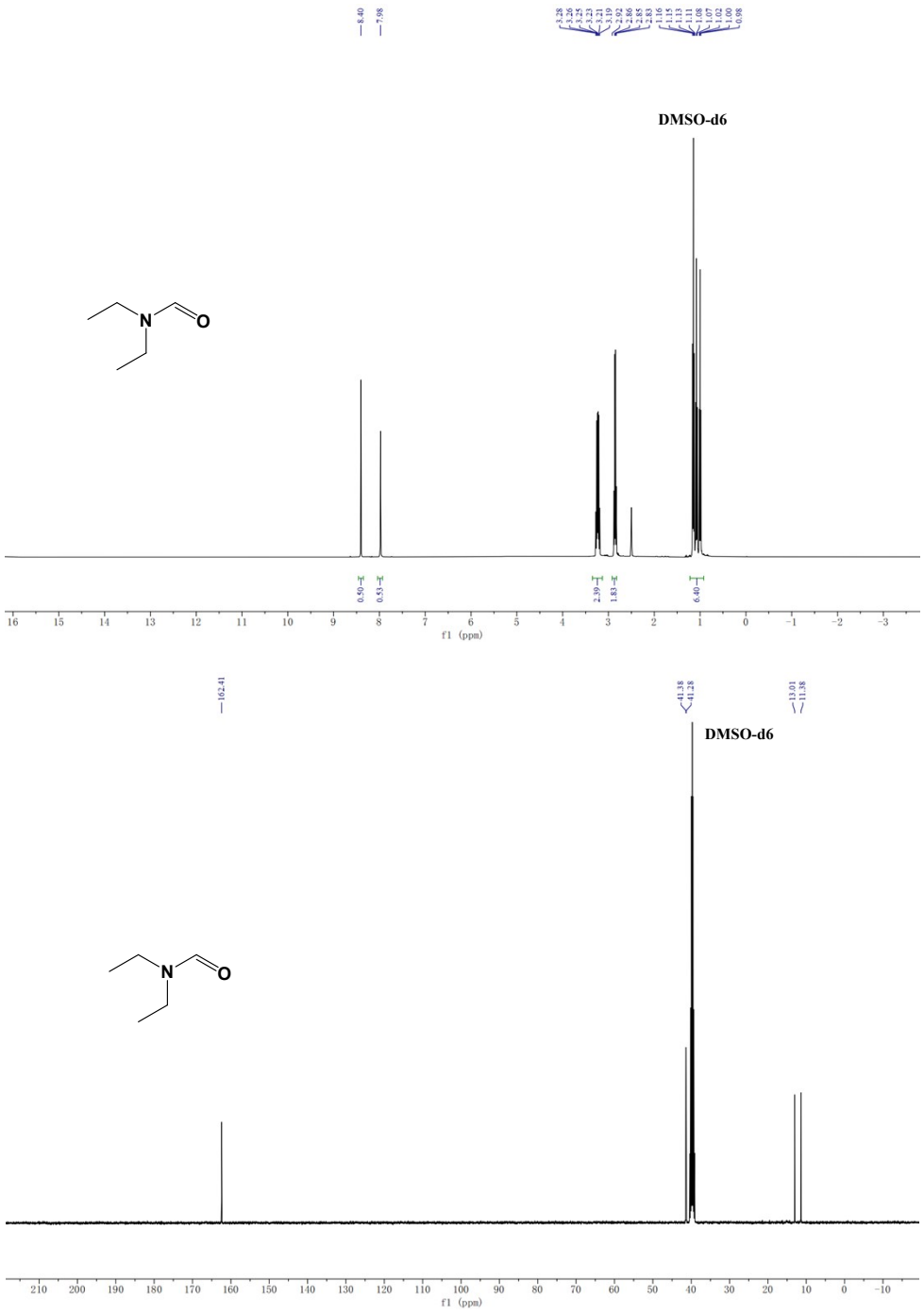

Fig. S11. ^{1}H NMR and ^{13}C NMR of N, N-diethylformamide in DMSO-d_6.

N, N-dibutylformamide, light yellow liquid, purification by column chromatography on silica gel using CH_2Cl_2/CH_3OH (50:1) as eluent. ^1H NMR (400 MHz, DMSO-d_6) δ 7.99 (s, 1H), 3.19 (q, J = 7.4 Hz, 4H), 1.43 (dt, J = 12.7, 7.3 Hz, 4H), 1.28-1.18 (m, 4H), 0.90-0.83 (m, 6H). ^{13}C NMR (151 MHz, DMSO-d_6) δ 162.68, 46.22, 40.94, 30.45, 29.15, 19.78, 18.64, 13.98, 13.84.

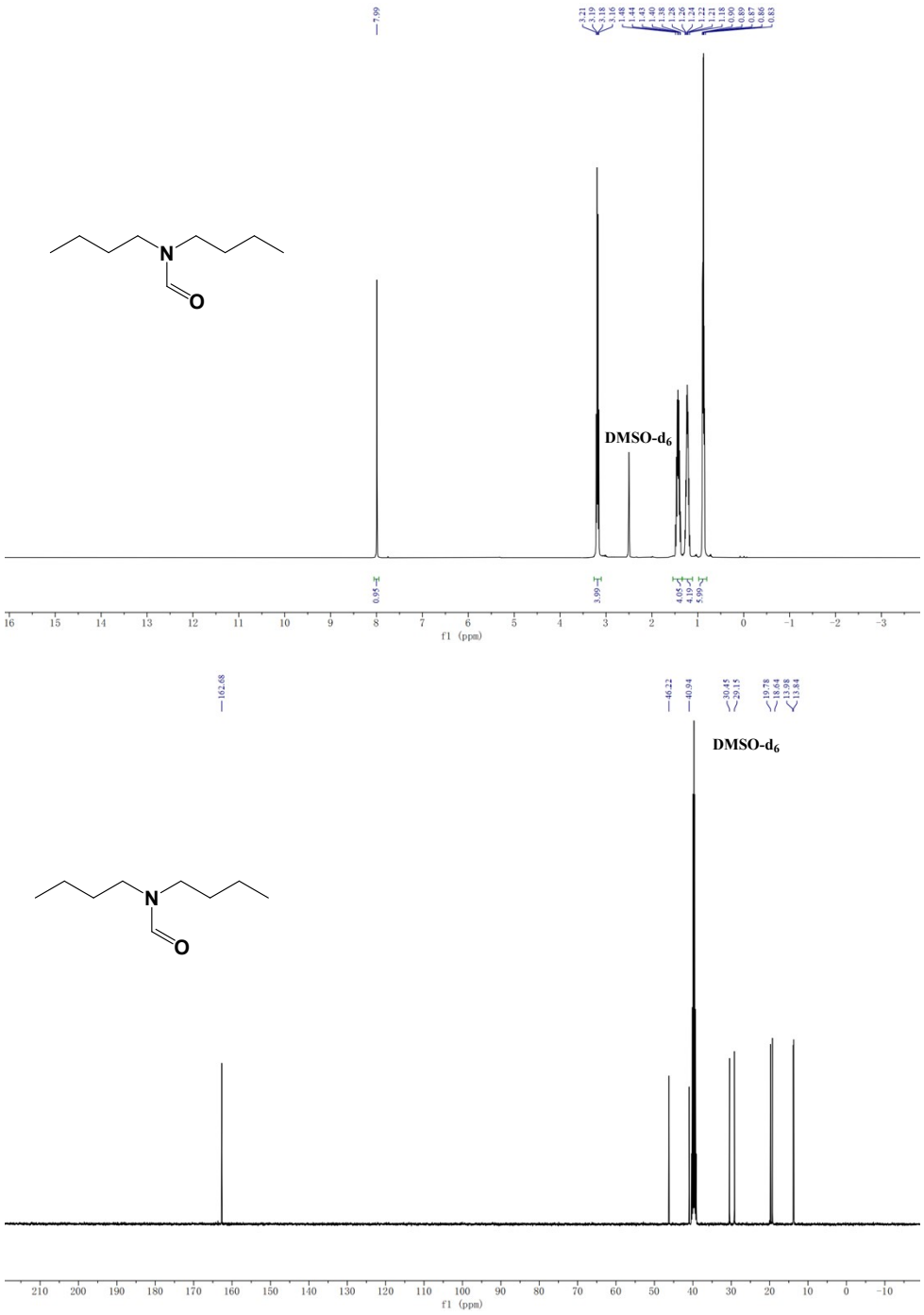

Fig. S12. ^1H NMR and ^{13}C NMR of N, N-dibutylformamide in DMSO-d_6.

N-formylpyrrolidine, colourless liquid, purification by reduced pressure distillation. ^{1}H NMR (400 MHz, $CDCl_3$) δ 8.20 (s, 1H), 3.48 (t, 2H), 3.38 (t, 2H), 1.88 (p, 4H). ^{13}C NMR (151 MHz, $CDCl_3$) δ 161.13, 45.77, 43.02, 24.71, 24.02.

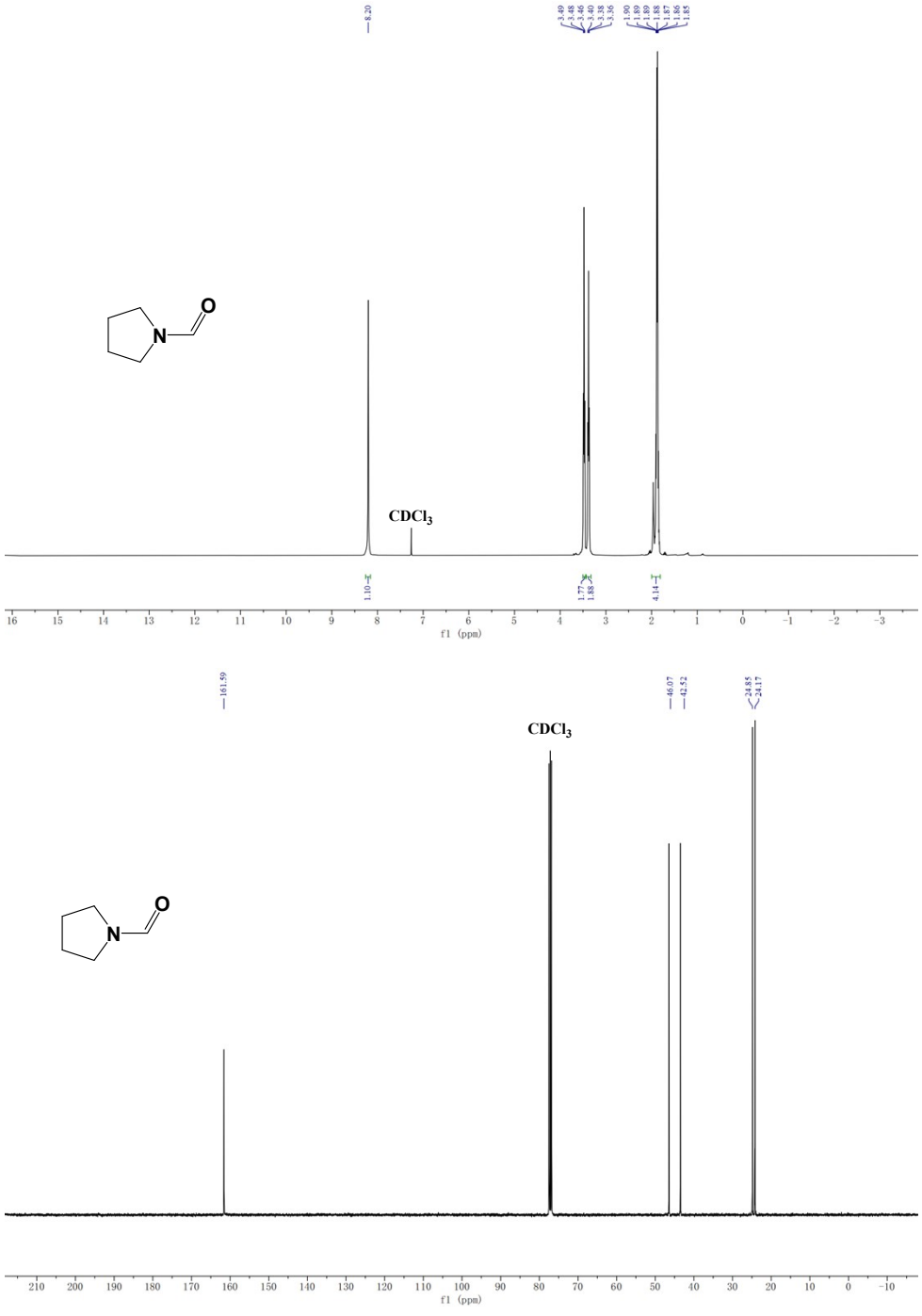

Fig. S13. ^{1}H NMR and ^{13}C NMR of N-formylpyrrolidine in $CDCl_3$.

N-formylpiperidine, colourless liquid, purification by column chromatography on silica gel using CH_2Cl_2/CH_3OH (10:1) as eluent. ^1H NMR (400 MHz, DMSO-d_6) δ 7.94 (s, 1H), 3.31 (dt, J = 15.9, 5.6 Hz, 4H), 1.62 (p, J = 5.7 Hz, 2H), 1.43 (dp, J = 22.9, 5.9 Hz, 4H). ^{13}C NMR (151 MHz, DMSO-d_6) δ 160.45, 47.66, 39.32, 26.43, 24.72, 24.06.

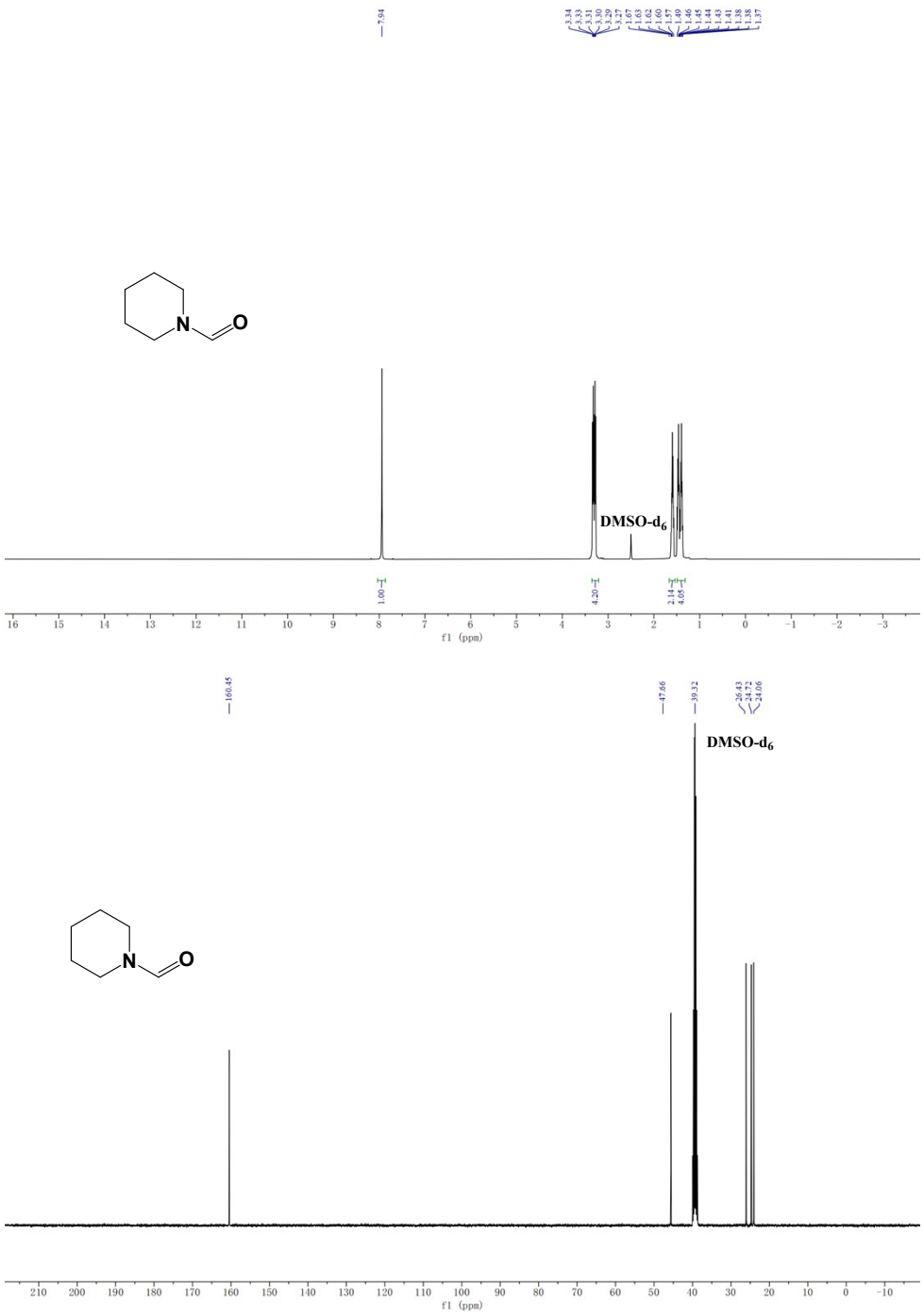

Fig. S14. ^1H NMR and ^{13}C NMR of N-formylpiperidine in DMSO-d_6.

N-propylformamide, light yellow liquid, purification by column chromatography on silica gel using CH_2Cl_2/CH_3OH (50:1) as eluent. ^1H NMR (400 MHz, DMSO-d_6) δ 8.20 (s, 1H), 3.02 (q, J = 6.8 Hz, 2H), 1.40 (h, J = 7.3 Hz, 2H), 0.83 (t, J = 7.4 Hz, 3H). ^{13}C NMR (151 MHz, DMSO-d_6) δ 161.22, 39.10, 22.60, 11.43.

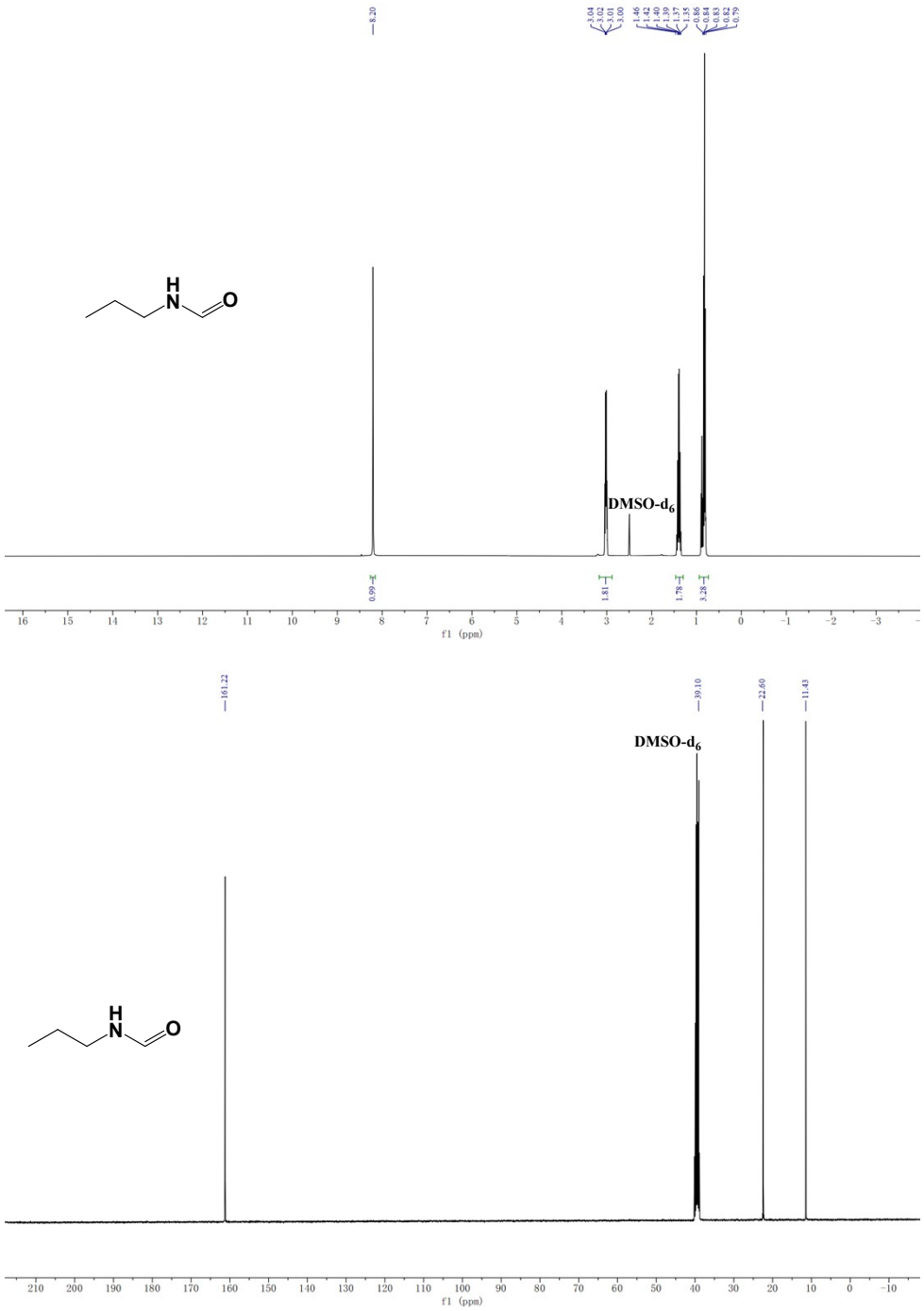

Fig. S15. ^1H NMR and ^{13}C NMR of N-propylformamide in DMSO-d_6.

N-cyclohexylformamide, white crystalline powder, purification by recrystallization in ether. ^{1}H NMR (400 MHz, DMSO-d_6) δ 8.45 (s, 1H), 2.88-2.81 (m, 1H), 1.87 (m, 2H), 1.69 (m, 2H), 1.26-1.04 (m, 6H). ^{13}C NMR (151 MHz, DMSO-d_6) δ 159.96, 46.22, 33.23, 31.34, 25.20, 24.48.

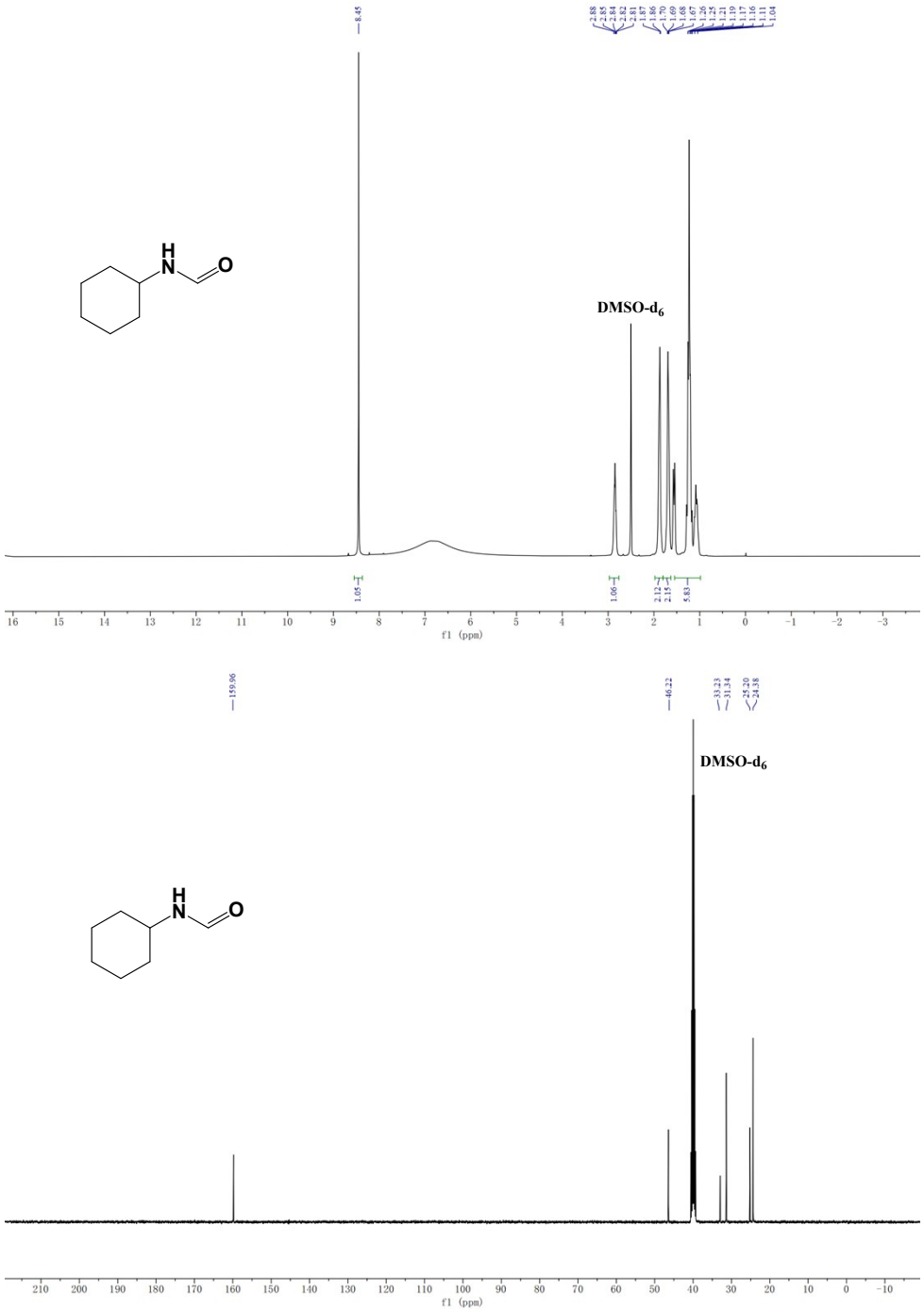

Fig. S16. ^{1}H NMR and ^{13}C NMR of N-cyclohexylformamide in DMSO-d_6.

N-benzylformamide, yellowish solid, purification by recrystallization in ether. ^{1}H NMR (400 MHz, $CDCl_3$) δ 8.24 (s, 1H), 7.46-7.28 (m, 5H), 4.47 (d, 2H). ^{13}C NMR (151 MHz, $CDCl_3$) δ 161.19, 137.69, 128.85, 127.86, 127.06, 42.23.

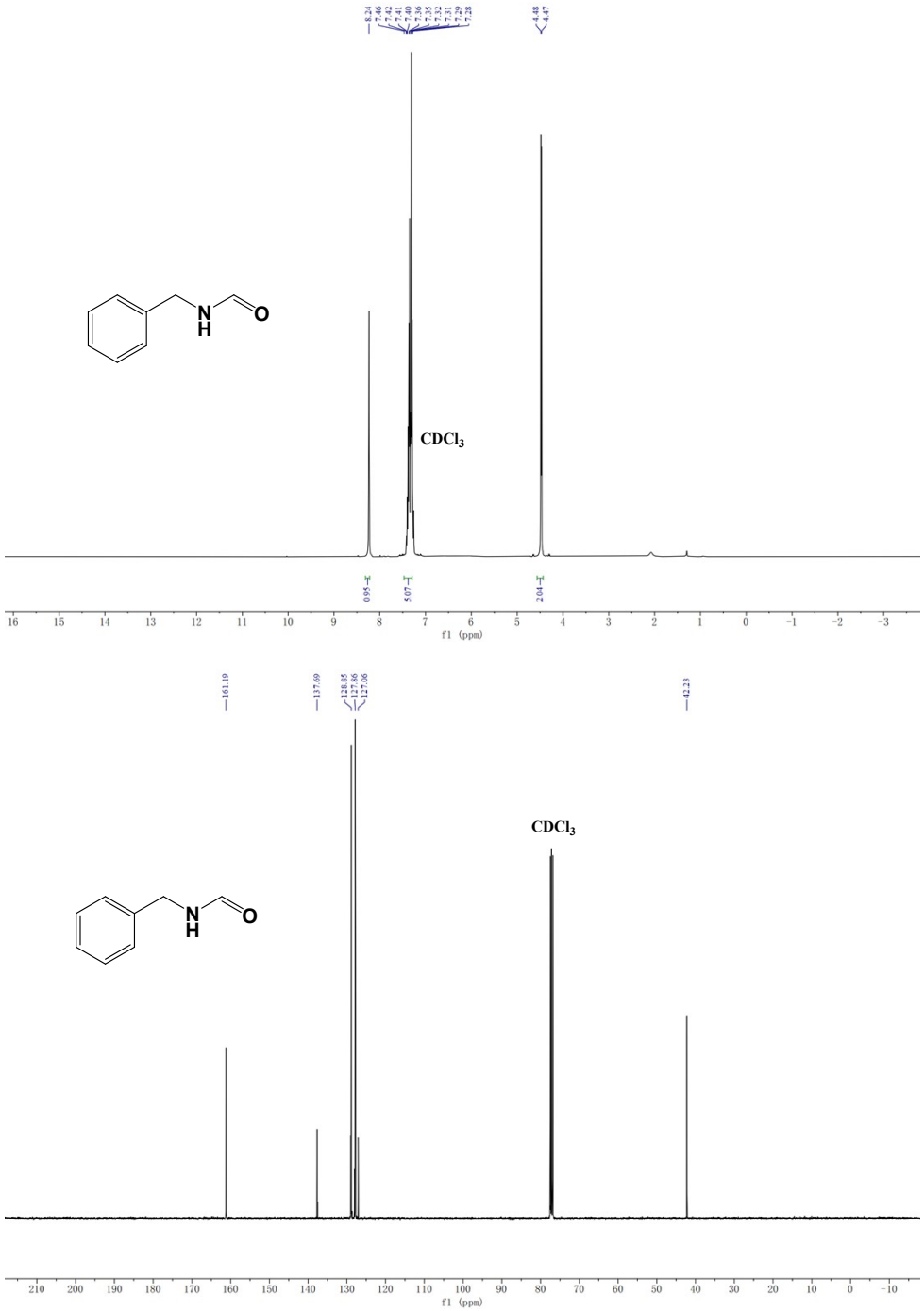

Fig. S17. ^{1}H NMR and ^{13}C NMR of N- benzylformamide in $CDCl_3$.

References

1 C. M. Tourné, G. F. Tourné, S. A. Malik, T. J. R. Weakley, J. *Inorg. Nucl. Chem.*, 1970, **32**, 3875-3890. https://doi.org/10.1016/0022-1902(70)80566-8

2 G. Herve, A. Teze. *Inorg. Chem.*, 1977, **16**, 2115-2117. https://doi.org/10.1021/ic50174a060

3 Y. Ma, Y. Jiang, X. Wei, Q. Peng, S. Dai, Z. Hou, *ACS Sustainable Chem. Eng.*, 2022, **10**, 15389–15401. https://doi.org/10.1021/acssuschemeng.2c04089

4 L. Bi, U. Kortz, B. Keita, L. Nadjo, H. Borrmann, *Inorg. Chem.*, 2004, **43**, 8367-8372. https://doi.org/10.1021/ic048864z

5 Y. Zhang, H. Wang, H. Yuan, and F. Shi, *ACS Sustainable Chem. Eng.*, 2017, **5**, 5758−5765. https://doi.org/10.1021/acssuschemeng.7b00363

6 Y. Wang, B. Chen, S. Liu, X. Shen, S. Li, Y. Yang, H. Liu, B. Han, *ChemCatChem*, 2018, **10**, 5124-5127. https://doi.org/10.1002/cctc.201801404

7 P. Ju, J. Chen, A. Chen, L. Chen, Y. Yu, *ACS Sustainable Chem. Eng.*, 2017, **5**, 2516-2528. https://doi.org/10.1021/acssuschemeng.6b02865

8 X. Cui, Y. Zhang, Y. Deng, F. Shi, *Chem. Commun.*, 2014, **50**, 189-191. https://doi.org/10.1039/C3CC46427J

9 X. Yu, Z. Yang, S. Guo, Z. Liu, H. Zhang, B. Yu, Y. Zhao, Z. Liu, *Chem. Commun.*, 2018, **54**, 7633-7636. https://doi.org/10.1039/C8CC03346C

10 T. Mitsudome, T. Urayama, S. Fujita, Z. Maeno, T. Mizugaki, K. Jitsukawa, K. Kaneda, ChemCatChem, 2017, **9**, 3632 – 3636. https://doi.org/ 10.1002/cctc. 201700726

11 Z. Yang, H. Wang, G. Ji, X. Yu, Y. Chen, X. Liu, C. Wu, Z. Liu, New J. Chem., 2017, **41**, 2869-2872. https://doi.org/10.1039/C6NJ03899A

12 D. Cheng, M. Wang, L. Tang, Z. Gao, X. Qin, Y. Gao, D. Xiao, W. Zhou, D. Ma, *Angew. Chem. Int. Ed.*, 2022, **61**, e202202654. https://doi.org/10.1002/anie.202202654

13 H. Liao, Y. Jiang, X. Wei, X. Zhao, W. Lai, N. An, Y. Ma, S. Dai, Z. Hou, *ACS Sustainable Chem. Eng.*, 2024, **12**, 2632-2645. https://doi.org/10.1039/C6NJ03899A